A COMPUTATIONAL EVALUATION OF TWO HIGH-RESOLUTION CONVECTIVE SCHEMES FOR PROBLEMS IN FLUID DYNAMICS

Miguel Antonio Caro Candezano, mcaro@icmc.usp.br
Patrícia Sartori, psartori@icmc.usp.br
Laís Corrêa, lacorrea@icmc.usp.br
Giseli Aparecida Braz de Lima, giabl@icmc.usp.br
Valdemir Garcia Ferreira, pvgf@icmc.usp.br
Instituto de Ciências Matemáticas e de Computação - USP, Fone: (16) 3373-9676, Av. Trabalhador são-carlense, 400 - CEP: 13560-970 - São Carlos - SP

Abstract. *It is well recognized that researchers face many problems for numerically approximating nonlinear convective terms in conservation laws and related fluid dynamics problems. One of the main challenges is to develop upwind schemes that capture well discontinuities (or shock waves) and allow high (at least second order) accuracy solution. In this scenario, the goal of this work is to present a computational evaluation of two genuinely Brazilian high resolution convective upwind schemes, namely ADBQUICKEST and SDPUS-C1, for solving general fluid dynamics problems. Both schemes are developed in the context of normalized variables (NV) of Leonard and satisfy the total-variation diminishing (TVD) constraints of Harten.*

Keywords: *convective terms, high resolution schemes, conservation laws, upwinding*

1. INTRODUCTION

To solve related problems of fluid dynamics using the classical convective schemes (e.g. FOU, CD, MINMOD, SUPERBEE) some imperfections can be developed in modeling convective terms, namely: diffusion, spurious oscillations, incorrect capture of shocks. To solve this kind of problems new high resolution upwind schemes are being proposed based on the NV, convection-boundedness criterion (CBC) and TVD concepts. In the literature, there is another approach to model the convective terms, such that ENO (Harten et al., 1987) and WENO (Liu et al., 1994) schemes that have robust shock capturing ability and high order of accuracy. However, this type of schemes are very cost and complicated implementation. In this paper, an implementation of two genuinely Brazilian high resolution upwind schemes, ADaptative Bounded QUICKEST (ADBQUICKEST) and Six-Degree Polynomial Upwind Scheme of C^1 class (SDPUS-C1) (both developed on the LCAD-ICMC/USP), is presented to solve some problems of fluid dynamics: 1D Burgers equation, 2D Euler, 2D shallow water and 2D Magnetohydrodynamics equations. Then, as application, these schemes are used for simulating incompressible fluid flow modeled by axisymmetric Navier-Stokes equations.

2. THEORETICAL BASE FOR THE DEVELOPMENT OF AN UPWIND SCHEME

We consider the 1D model for advection of a scalar

$$\phi_t + a\phi_x = 0, \quad a = \text{const.} > 0, \tag{1}$$

$$\phi(x,0) = \phi_0(x), \quad x \in \mathbb{R},$$

with the analytical solution given by $\phi(x) = \phi(x - at)$. The numerical approximation for (1) using the conservative finite difference methodology is

$$\phi_i^{n+1} = \phi_i^n - \theta(\phi_{i+1/2}^n - \phi_{i-1/2}^n), \tag{2}$$

where ϕ_i^n is the numerical solution at mesh point $(i\delta x, n\delta t)$; δx and δt are the space and time increments, respectively. $\theta = a\delta t/\delta x$ is the Courant-Friedrichs-Lewy (CFL) number. The quantities $\phi_{i+1/2}^n$ and $\phi_{i-1/2}^n$ are the numerical flux functions, which depend on three selected neighboring mesh points, namely D (Downstream), U (Upstream) and R (Remote-upstream), that are determined according to the convective velocity V_f at the faces $i + 1/2$ or $i - 1/2$, as show in Fig. 1. In this manner, the

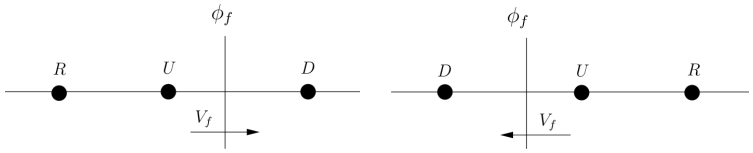

(a) $V_f > 0$ (b) $V_f < 0$

Figure 1. Position of computational nodes D, U and R according to the sign of V_f speed of a convective variable ϕ_f.

variable ϕ is transformed into the NV of Leonard (1988) by $\hat{\phi_{()}} = \frac{\phi_{()} - \phi_R}{\phi_D - \phi_R}$. The advantage of this new formulation is that interface value $\hat{\phi}_f$ depends on $\hat{\phi}_U$ only, since $\hat{\phi}_D = 1$ and $\hat{\phi}_R = 0$. In this context, it is possible to derive a nonlinear monotonic NV scheme by imposing the following conditions for $0 \leq \hat{\phi}_U \leq 1$: $\hat{\phi}_f(0) = 0$ (a necessary condition), $\hat{\phi}_f(1) = 1$ (a necessary condition), $\hat{\phi}_f(0.5) = 0.75$ (a necessary and sufficient condition to reach second order of accuracy) and $\hat{\phi}'_f(0.5) = 0.75$ (a necessary and sufficient condition to reach third order of accuracy). Leonard (1988) also recommends that for values of $\hat{\phi}_U < 0$ or $\hat{\phi}_U > 1$, the scheme must be extended using the FOU (First Order Upwinding) scheme, which is defined by $\hat{\phi}_f = \hat{\phi}_U$.

After deriving a scheme in NV, it is possible to rewrite it in the form of the flux limiter from the relationship $\hat{\phi}_f = \hat{\phi}_U + \frac{1}{2}\psi(r_f)(1 - \hat{\phi}_U)$, where $\psi(r_f) = \psi_f$ is the flux limiter function and r_f is the reason of two consecutive gradients (a sensor), given by $r_f = \frac{1}{1-\hat{\phi}_U}$.

To ensure limited solution (stability) we consider the CBC of Gaskell and Lau (1988), as follows

$$\begin{aligned} &\hat{\phi}_U \leq \hat{\phi}_f(\hat{\phi}_U) \leq 1, \qquad \text{if } \hat{\phi}_U \in [0,1]; \\ &\hat{\phi}_f = \hat{\phi}_f(\hat{\phi}_U) = \hat{\phi}_U, \qquad \text{if } \hat{\phi}_U \notin [0,1]; \\ &\hat{\phi}_f(0) = 0 \quad \text{and} \quad \hat{\phi}_f(1) = 1. \end{aligned} \tag{3}$$

Another important stability criterion is the TVD constraint of Harten (1983). This property ensures that, in general, spurious oscillations (unphysical noises) are removed from the numerical solution. Formally, we consider a sequence of discrete approximations $\phi(t) = \phi_i(t)_{i\in\mathbb{Z}}$ for a scalar quantity. The total variation (TV) at time t of this sequence is defined by $TV(\phi(t)) = \sum_{i\in\mathbb{Z}} |\phi_{i+1}(t) - \phi_i(t)|$. From this definition, we say that the scheme is TVD if, for all data set ϕ^n, the values ϕ^{n+1} calculated by numerical method satisfy

$$TV(\phi^{n+1}) \leq TV(\phi^n), \quad \forall n. \tag{4}$$

It is important to emphasize, from numerical point of view, that TVD schemes are very attractive, since they guarantee convergence, monotonicity and high accuracy.

3. THE UPWIND SCHEMES

In this section we briefly describe two high resolution upwind schemes implemented in this work.

3.1 ADBQUICKEST:

It is a high resolution upwind scheme developed by Ferreira (2009), that depends of the time parameter θ and is defined by

$$\hat{\phi}_f = \begin{cases} (2-|\theta|)\hat{\phi}_U, & \text{if } 0 < \hat{\phi}_U < a, \\ \hat{\phi}_U + \frac{1}{2}(1-|\theta|)(1-\hat{\phi}_U) - \frac{1}{6}(1-\theta^2)(1-2\hat{\phi}_U), & \text{if } a \le \hat{\phi}_U \le b, \\ 1-|\theta|+|\theta|\hat{\phi}_U, & \text{if } b < \hat{\phi}_U < 1, \\ \hat{\phi}_U, & \text{otherwise,} \end{cases} \tag{5}$$

where $a = \frac{2-3|\theta|+\theta^2}{7-9|\theta|+2\theta^2}$ and $b = \frac{-4+3|\theta|+\theta^2}{-5+3|\theta|+2\theta^2}$. The flux limiter of ADBQUICKEST scheme is given by

$$\psi(r_f) = \max\left\{0,\ \min\left[2r_f, \frac{2+\theta^2-3|\theta|+(1-\theta^2)r_f}{3-3|\theta|}, 2\right]\right\}. \tag{6}$$

3.2 SDPUS-C1:

This high resolution upwind scheme is based in a six-degree polynomial developed by Lima (2010) that depends of a free parameter $\alpha \in [4, 12]$. For this polynomial interpolation the best results are obtained with $\alpha = 12$. In NV the scheme is defined by

$$\hat{\phi}_f = \begin{cases} (-24+4\alpha)\hat{\phi}_U^6 + (68-12\alpha)\hat{\phi}_U^5 + (-64+13\alpha)\hat{\phi}_U^4 + (20-6\alpha)\hat{\phi}_U^3 + \alpha\hat{\phi}_U^2 + \hat{\phi}_U, & \text{if } \hat{\phi}_U \in [0,1]; \\ \hat{\phi}_U, & \text{if } \hat{\phi}_U \notin [0,1]. \end{cases} \tag{7}$$

The flux limiter of this scheme is

$$\psi(r_f) = \max\left\{0,\ \frac{0.5(|r_f|+r_f)[(-8+2\alpha)r_f^3 + (40-4\alpha)r_f^2 + 2\alpha r_f]}{(1+|r_f|)^5}\right\}. \tag{8}$$

4. NUMERICAL RESULTS

In order to evaluate the performance of the ADBQUICKEST and SDPUS-C1 high resolution upwind schemes, we consider nonlinear hyperbolic conservation laws, such as the 1D Burgers equation, 2D Euler, 2D shallow water and 2D MHD equations. Then, as application, these schemes are used for simulating incompressible fluid flow modeled by axisymmetric Navier-Stokes equations.

4.1 1D Burgers equation

The nonlinear Burgers equation is a PDE that can be viewed as a nonlinear wave, where every point on the wave front can propagate with a different speed (ϕ). This equation is given by $\phi_t + (\frac{1}{2}\phi^2)_x = 0$, where ϕ is the conserved variable and $\frac{1}{2}\phi^2$ is the flux function. The initial condition and exact solution for this problem, respectively, are given by

$$\phi_0(x) = \begin{cases} 1, & \text{if } |x| < \frac{1}{3}; \\ -1, & \text{if } \frac{1}{3} < |x| \le 1; \end{cases} \quad \text{and} \quad \phi(x) = \begin{cases} -1, & \text{if } x < -t - \frac{1}{3}; \\ \frac{x+\frac{1}{3}}{t}, & \text{if } -t-\frac{1}{3} < x < t - \frac{1}{3}; \\ 1, & \text{if } t - \frac{1}{3} < x < \frac{1}{3}; \\ -1, & \text{if } x > \frac{1}{3}. \end{cases} \tag{9}$$

This problem is characterized by a rarefaction wave with presence of a sonic point at $\phi = 0$, where the wave speed changes sign, as ϕ varies from -1 to 1. In this region, numerical difficulties called sonic glitch may arise, in that a local extreme is created and the solution is not monotone along of the transonic rarefaction. In the literature, to cure the sonic glitch is recommended to apply an entropy fix to add numerical viscosity in the finite-difference scheme (we use Harten's entropy fix). From Fig. 2 (a), we can see that high resolution upwind schemes, studied here, fail to capture the rarefaction wave generating an unphysical expansion shock. On the other hand, in Fig. 2 (b) with the implementation of Harten's entropy fix, both schemes present dissipations around the corners at the head and tail of the expansion wave, but capture satisfactorily the shock. In this test, we can say that SDPUS-C1 scheme models a little better the problem than ADBQUICKEST scheme.

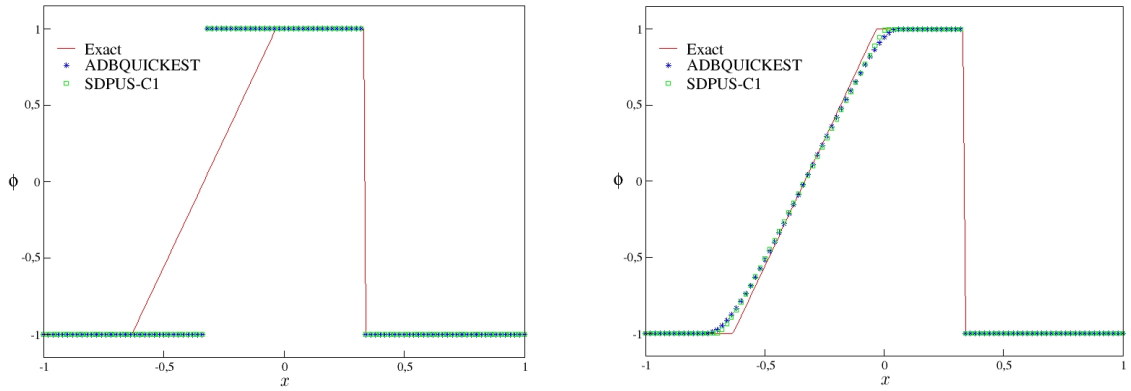

(a) (b)

Figure 2. The exact and computed solutions of inviscid Burgers equation with sonic point implementing the ADBQUICKEST and SDPUS-C1 schemes with 200 cells, $\theta = 0.5$ at $t = 0.3$: (a) without a Harten's entropy fix and (b) with Harten's entropy fix

4.2 2D Euler equations

The Euler equations govern the dynamic of a compressible material, such as gases or liquids at high pressures, for which the effects of body forces, viscous stresses and heat flux are neglected. These equations are given by $\phi_t + F(\phi)_x + G(\phi)_y = 0$, where $\phi = [\rho, \rho u, \rho v, E]^T$ is the conserved variable vector, $F(\phi) = [\rho u, \rho u^2 + p, \rho uv, (E + p)u]^T$ and $G(\phi) = [\rho v, \rho uv, \rho v^2 + p, (E + p)v]^T$ are the flux function vectors, with ρ the density, $[\rho u, \rho v]^T$ the momentum vector, E the total energy and p the pressure. To close the system, we consider the ideal gas equation $p = (\lambda - 1)(E - \frac{1}{2}\rho(u^2 + v^2))$, where $\lambda = 1.4$ is the ratio of specific heats. The Euler equations are supplemented with the following initial conditions that correspond to shock-shock interaction problem (see LeVeque (2002))

$$[\rho_0,\ u_0,\ v_0,\ p_0]^T = \begin{cases} [1.5,\ 0,\ 0,\ 1.5]^T, & \text{state a;} \\ [0.13799,\ 1.2060454,\ 1.2060454,\ 0.0290323]^T, & \text{state b;} \\ [0.5322581,\ 1.2060454,\ 0,\ 0.3]^T, & \text{state c;} \\ [0.5322581,\ 0,\ 1.2060454,\ 0.3]^T, & \text{state d.} \end{cases} \tag{10}$$

The numerical solutions of this problem are calculated with the `CLAWPACK` software developed by LeVeque, using the Godunov method with correction term, where are added the flux limiters of ADBQUICKEST and SDPUS-C1 schemes with $\theta = 0.8$, a mesh of 200×200 cells at $t = 0.8$. The reference solution is computed with the Godunov method implementing the monotonized center (MC) limiter and $\theta = 0.5$. Figure 3 presents the results for ρ contours and Fig. 4 depicts ρ variation on the $y = x$. It can be seen that both schemes are in good agreement with the reference solution, being that SDPUS-C1 scheme provided the best results.

4.3 2D Shallow water equations

The 2D shallow water equations are given by $\phi_t + F(\phi)_x + G(\phi)_y = 0$, where $\phi = [h, hu, hv]^T$ is the conserved variable vector, $F(\phi) = [hu, hu^2 + \frac{1}{2}gh^2, huv]^T$ and $G(\phi) = [hu, huv, hv^2 + \frac{1}{2}gh^2]^T$ are the flux functions vectors, in which h represents the height of fluid, $[u, v]^T$ and $[hu, hv]^T$ are, respectively, the velocity and discharge vectors, and g is the acceleration due to gravity. In order to verify the performance of ADBQUICKEST and SDPUS-C1 schemes, we simulate a radial dam-break problem (see, for instance, LeVeque (2002)). In summary, this problem models a dam, initially at rest, dividing the domain $\Omega = [-2.5, 2.5] \times [-2.5, 2.5]$ in two parts (inside of the dam and outside of it). At $t = 0$, the dam is removed forming a shock wave, that travels radially outwards while a rarefaction wave propagates inwards. This problem is illustrated in Fig. (5) (case (a) at $t = 0$ and case

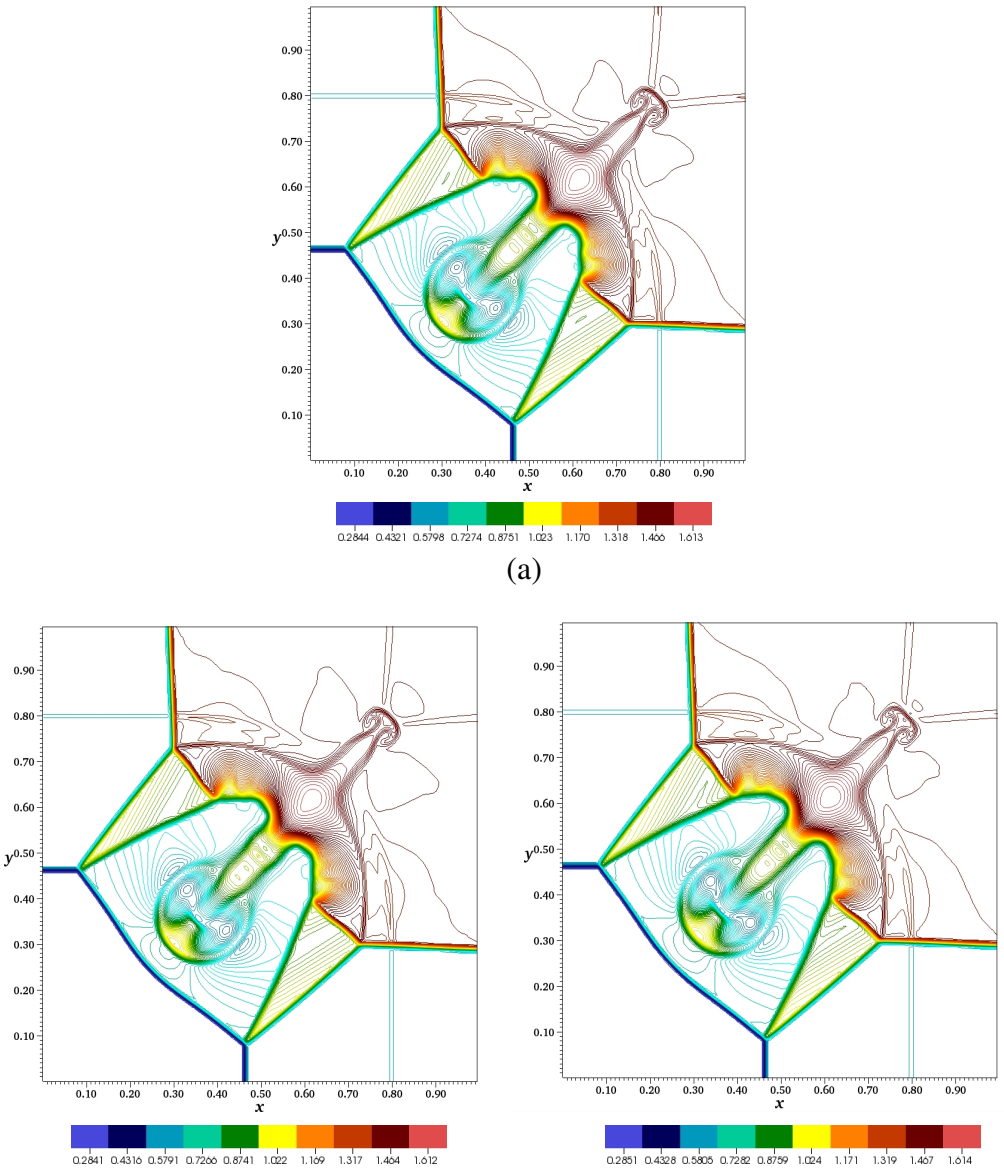

Figure 3. The computed solutions for shock-shock interation problem (ρ- contours) with a mesh size of 200×200 cells at $t = 0.8$: (a) Reference with $\theta = 0.5$, (b) ADBQUICKEST and (c) SDPUS-C1 with $\theta = 0.8$

(b) at $t = 0.25$), where the depth is initially $h = 2$ inside a dam and $h = 1$ outside. To simulate this problem we use too the `CLAWPACK` software, in that the numerical solutions are obtained implementing ADBQUICKEST and SDPUS-C1 schemes with a mesh size of 125×125 cells and $\theta = 0.8$. The reference solution is calculated with mesh size of 250×250 cells and $\theta = 0.5$. The simulation for h profile (cross section), at $x \perp y$ plane at $t = 1.5$, is depicted in Fig. (6).

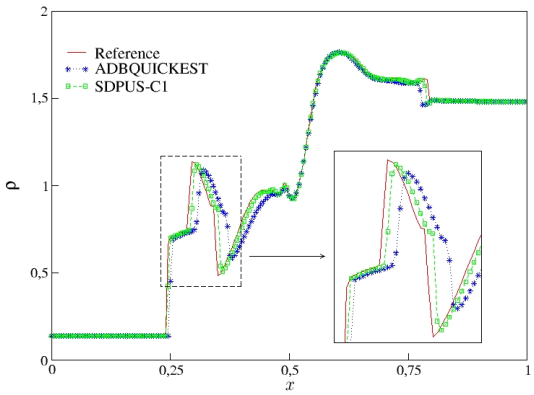

Figure 4. Comparison between reference and computed solutions with the ADBQUICKEST and SDPUS-C1 upwind schemes at $t = 0.8$ to the ρ variation in $y = x$

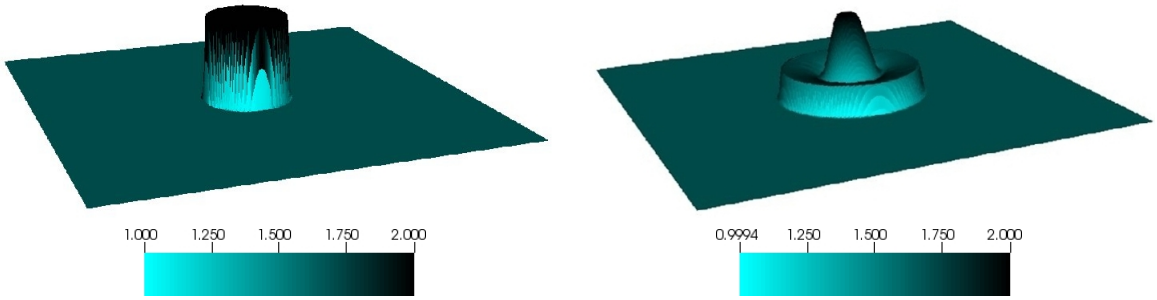

(a) (b)

Figure 5. The radial dam-break problem at (a) $t = 0$ and (b) $t = 0.25$

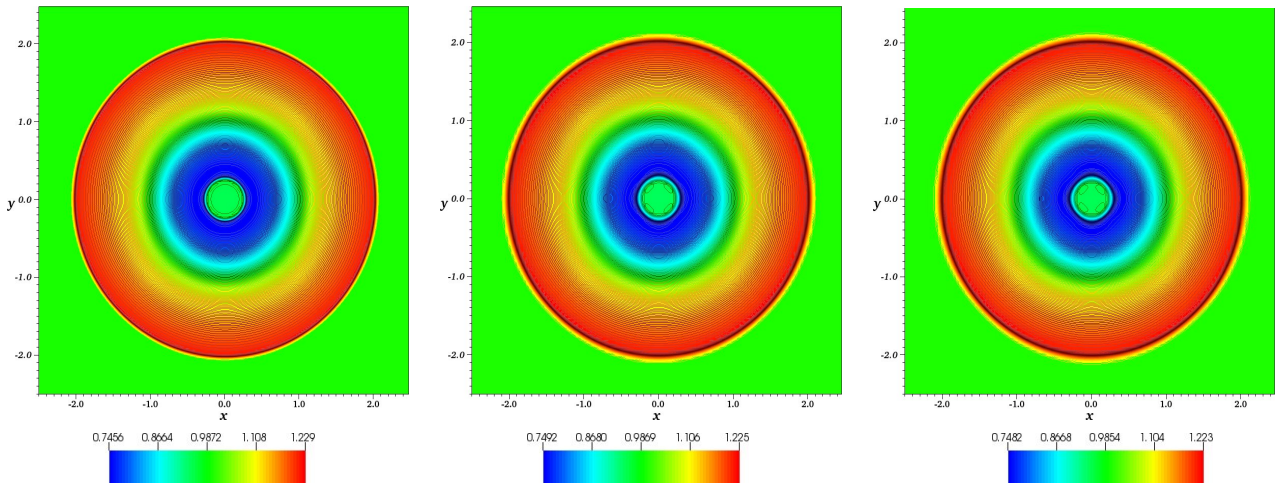

(a) (b) (c)

Figure 6. Radial dam-break problem at $t = 1.5$: (a) h profiles for reference solution with a mesh size of 250×250 cells and $\theta = 0.5$, (b) h profiles for ADBQUICKEST and (c) h profiles for SDPUS-C1 with a mesh size of 125×125 cells and $\theta = 0.8$

To complete the analysis, we compute the depth variation as a function of distance from the origin (e.g. h in $y = 0$), as is shown in Fig. (7). We see that results are in agreement with the reference solution.

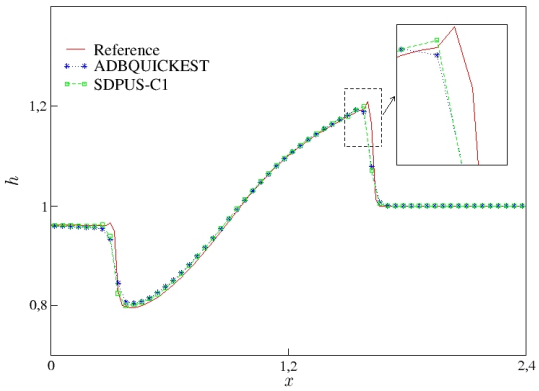

Figure 7. Comparison between reference and computed solutions with the ADBQUICKEST and SDPUS-C1 schemes at $t = 1.5$ to the h variation in $y = 0$

4.4 2D Magnetohydrodynamics equations

The ideal MHD equations are a nonlinear system of hyperbolic conservation laws that characterize the flow of a conducting fluid in a presence of magnetic field. They are defined by

$$\begin{bmatrix} \rho \\ \rho\overrightarrow{u} \\ \mathcal{E} \\ \overrightarrow{\boldsymbol{B}} \end{bmatrix}_t + \overrightarrow{\nabla}\cdot \begin{bmatrix} \rho\overrightarrow{u} \\ \rho\overrightarrow{u}\otimes\overrightarrow{u} + \left(p + \frac{1}{2}|\overrightarrow{\boldsymbol{B}}|^2\right)\mathcal{I} - \overrightarrow{\boldsymbol{B}}\otimes\overrightarrow{\boldsymbol{B}} \\ \overrightarrow{u}(\mathcal{E} + p + \frac{1}{2}|\overrightarrow{\boldsymbol{B}}|^2) - \overrightarrow{\boldsymbol{B}}(\overrightarrow{u}\cdot\overrightarrow{\boldsymbol{B}}) \\ \overrightarrow{u}\otimes\overrightarrow{\boldsymbol{B}} - \overrightarrow{\boldsymbol{B}}\otimes\overrightarrow{u} \end{bmatrix} = 0, \tag{11}$$

where ρ is the density, $\overrightarrow{u} = (u_1, u_2, u_3)$ is the fluid velocity, $\mathcal{E} = \frac{1}{2}\rho u^2 + \frac{1}{2}B^2 + \frac{p}{(\gamma-1)}$ is the total energy, $\overrightarrow{\boldsymbol{B}} = (\boldsymbol{B}_1, \boldsymbol{B}_2.\boldsymbol{B}_3)$ is the magnetic field, p is the thermal pressure and $\frac{1}{2}|\boldsymbol{B}|^2$ is the magnetic pressure, $\gamma = 5/3$ is the ratio of the specific heats. The system has eight unknowns $\phi = (\rho, \rho\overrightarrow{u}, \mathcal{E}, \overrightarrow{\boldsymbol{B}})$ and eight equations. In addition of these equations, the magnetic field satisfies the free divergence condition, $\overrightarrow{\nabla}\cdot\overrightarrow{\boldsymbol{B}} = 0$.

4.4.1 The Orszag-Tang MHD Turbulence Problem

We present here the numerical solutions of two-dimensional MHD equations namely the Orszag-Tang Turbulence problem. This model describes the evolution of the vortex system involving the interaction between several shock's waves traveling at various speed regimes. This test is very attractive from the point of view of numerical experiments. The Orszag-Tang problem is implemented using `CLAWPACK` with ADBQUICKEST and SDPUS-C1 high resolution upwind schemes, in a domain of $[0, 2\pi] \times [0, 2\pi]$ with a grid of 256×256, at time $t = 3.0$ and $\theta = 0.75$. The initial conditions are given by: $\rho = \gamma^2, u_1 = -\sin y, u_2 = \sin x, u_3 = 0, B_1 = -\sin y, B_2 = sin2x, B_3 = 0, p = \gamma$. Figure 8 (a) and Fig. 8 (b) show that results at $t = 3$ agree with ones given by Jiang (1999). It can be seen that the evolution of the system is complex and many shocks of all kinds are formed. Figure 9 (a) and Fig. 9 (b) show the pressure distribution along a cut $y = 0.625\pi$ at $t = 3.0$. We can see that results obtained using ADBQUICKEST and SDPUS-C1 schemes are consistent with the reference solution (Balbás et al., 2004) at this time. The Table 1 shows the norm of errors and the order of accuracy (P) of ADBQUICKEST and SDPUS-C1 schemes at $t = 0.25$. The errors are calculated as the deviations of the density from its value obtained on a 512×512 grid points. Both schemes present almost similarly order of accuracy. As we can see, an increasing order of accuracy is expected when enough points are added. An important difference between two schemes in this implementation is that ADBQUICKEST scheme is cost computationally than SDPUS-C1 scheme.

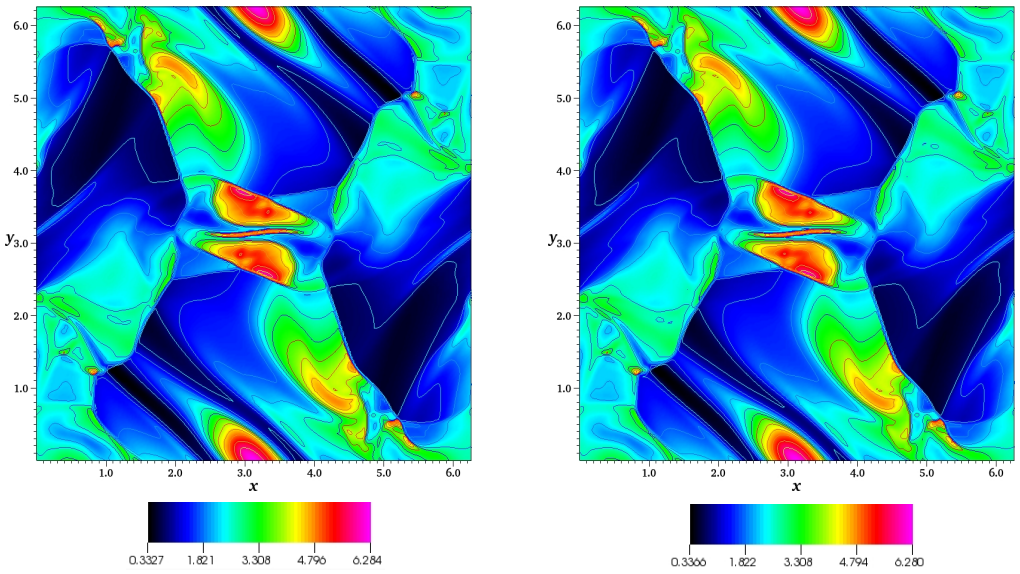

(a) (b)

Figure 8. The Orszag-Tang MHD Turbulence problem with a uniform 256×256 grid points, $\theta = 0.75$ at $t = 2.0$ for pressure with 12 contour lines: (a) ADBQUICKEST and (b) SDPUS-C1

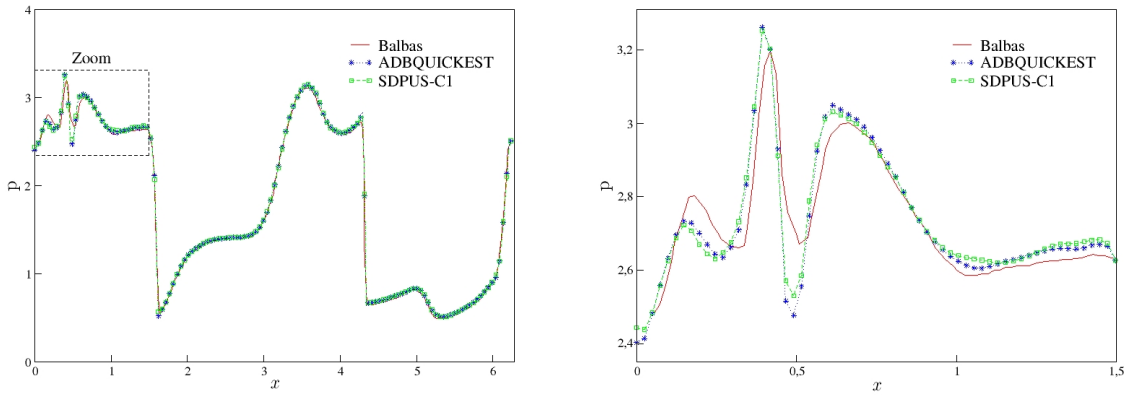

(a) (b)

Figure 9. The pressure distribution along a cut at $y = 0.625\pi$ for the Orszag-Tang MHD Turbulence problem at $t = 3.0$, where: (a) the reference (Balbás et al., 2004) and computed solutions with ADBQUICKEST and SDPUS-C1 schemes, and Fig. 9 (b) a Zoom

Table 1. Accuracy on the Orszag-Tang Turbulence problem using ADBQUICKEST and SDPUS-C1 schemes at $t = 0.25$.

Schemes	N	L_1		L_2	
		Error	P	Error	P
ADBQUICKEST	16	0.587397	—	0.273827	—
	32	0.277637	1.081136	0.135317	1.016923
	64	0.129196	1.103637	0.063776	1.085263
	128	0.054434	1.246984	0.027523	1.212381
	256	0.018197	1.580841	0.009172	1.585270
SDPUS-C1	16	0.587300	—	0.274211	—
	32	0.275491	1.092094	0.136417	1.007261
	64	0.128218	1.103404	0.063699	1.098677
	128	0.054878	1.224310	0.027682	1.202304
	256	0.018307	1.583823	0.009220	1.586121

4.5 Axisymmetric Navier-Stokes equations

These equations model incompressible fluid flow problems both in laminar and turbulent regimes. In the case of the fluid to be considered a homogeneous medium, the density of the particles does not vary during the movement and the transport properties are constant, the mathematical equations of physical conservation laws for simulation of laminar flows are the instantaneous Navier-Stokes and continuity equations, which in cylindrical coordinates system are given by

$$\frac{\partial u}{\partial t}+\frac{1}{r}\frac{\partial (ruu)}{\partial r}+\frac{\partial (uv)}{\partial z} = -\frac{\partial p}{\partial r}+\frac{1}{Re}\frac{\partial}{\partial z}\left(\frac{\partial u}{\partial z}-\frac{\partial v}{\partial r}\right)+\frac{1}{Fr^2}g_r, \tag{12}$$

$$\frac{\partial v}{\partial t}+\frac{1}{r}\frac{\partial (rvu)}{\partial r}+\frac{\partial (vv)}{\partial z} = -\frac{\partial p}{\partial z}+\frac{1}{Re}\frac{1}{r}\frac{\partial}{\partial r}\left(r\frac{\partial u}{\partial z}-\frac{\partial v}{\partial r}\right)+\frac{1}{Fr^2}g_z, \tag{13}$$

$$\frac{1}{r}\frac{\partial (ru)}{\partial r}+\frac{\partial v}{\partial z} = 0, \tag{14}$$

where t is time, $u=u(r,z,t)$ and $v=v(r,z,t)$ are, respectively, the components of velocity vector in the r and z directions, $g=(g_r,g_z)^T$ is the acceleration due to gravity, with $g_r=0m/s^2$ and $g_z=9.81m/s^2$, and p is the pressure (more specifically, pressure divided by density). The dimensionless parameters $Re=U_0L_0/\nu$ and $Fr=U_0/\sqrt{L_0g}$ represent, respectively, the Reynolds and Froud numbers, ν being the coefficient of kinematic viscosity given by $\nu=\frac{\mu}{\rho}$, where μ is the dynamic viscosity. Finally, U_0 and L_0 are characteristic scales for velocity and length, respectively.

Equations (12), (13) and (14) are applied for solving the problem of a vertical free jet penetrating into a recipient with the same fluid at rest, and it was realized by Taylor (1974). We use this problem to validate our numerical method, using the Freeflow code, developed by Castelo et al. (2000), equipped with ADBQUICKEST and SDPUS-C1 schemes. For the simulation of this incompressible flow involving free surfaces, we consider a cylindrical container with $0.06m$ of radius and $0.17m$ in height; the fluid inside container possesses $0.16m$ of height and the injector, with $0.03m$ in height and $0.002m$ of radius, is positioned at $0.1m$ from the free surface of the fluid at rest. The scales involved are $U_0=0.5m/s$ and $L_0=0.004m$. The dimensionless Reynolds and Froude numbers are $Re=200$ and $Fr=2.52409$ respectively. Figure (10) shows (a) experimental results, (b) and (c) the numerical results at time $t=2.5s$. From these figures one can see that the physics of the problem is successfully simulated. Moreover, the implementation of these high resolution upwind schemes, ADBQUICKEST and SDPUS-C1, is able to efficaciously capture the irregularities present on the free surface of fluid.

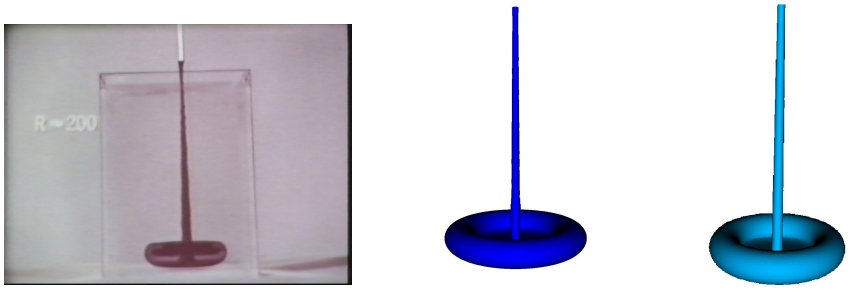

(a) (b) (c)

Figure 10. Comparison of (a) experimental results at $t=2.5s$ and numerical results obtained in the fluid vertical jet problem for $Re=200$ at $t=2.5s$ by (b) ADBQUICKEST and (c) SDPUS-C1 schemes

5. CONCLUSION

In this paper we have presented an implementation of some problems of fluid dynamics 1D and 2D such as 1D Burgers equation, 2D Euler of gas dynamics, 2D shallow water, 2D ideal MHD equations

and an experiment modeled by axisymmetric Navier-Stokes equations. The convective terms are modeled using the ADBQUICKEST and SDPUS-C1 high resolution upwind schemes. The upwind implementation of mentioned above problems are in agreement with the literature and then we believe that these schemes offer a possibility to model this kind of problem with a good efficient in comparison with another schemes of the same type. In future works we will present a comparison of ENO/WENO schemes with new TVD upwind schemes that actually are been developed at the LCAD-ICMC/USP.

6. ACKNOWLEDGEMENTS

We gratefully acknowledge the support provided by FAPESP (Grants 2008/07367-9 and 2009/16954-8), CNPq (Grants 133446/2009-3, 300479/2008-5 and 573710/2008-2 (INCT-MACC)), CAPES (Grant PECPG1462/08-3) and FAPERJ (Grant E-26/170.030/2008 (INCT-MACC)).

7. REFERENCES

Balbás J., Tadmor E., Wu C., 2004, "Non-oscillatory central schemes for one- and two-dimensional MHD equations: I", Journal of Computational Physics, Vol. 201, pp. 261-285.

Castelo A., Tomé M.F., César C.N.L., McKee S. and Cuminato J.A., 2000, "Freeflow: an integrated simulation system for three-dimensional free surface flows", Journal of Computers and Visualization in Science, Vol. 2, pp. 199-210.

Ferreira, V.G., Kurokawa, F.A., Queiroz, R.A.B., Kaibara, M.K., Oishi, C.M., Cuminato, J.A., Castelo, A., Tomé, M.F. and McKee, S., 2009, "Assessment of a high-order finite difference upwind scheme for the simulation of convection-diffusion problems", International Journal for Numerical Methods in Fluids, Vol. 60, pp. 1-26.

Gaskell, P.H. and Lau, A.K.C., 1988, "Curvature-compensated convective transport: Smart, a new boundedness preserving transport algorithm", International Journal for Numerical Methods in Fluids, Vol. 8, pp. 617-641.

Harten, A., 1983, "High resolution schemes for hyperbolic conservation laws", Journal of Computational Physics, Vol. 49, pp. 357-393.

Harten, A., Engquist, B., Osher, S. and Chakravarthy, S., 1987, "Uniformly high-order accurate essentially non-oscillatory schemes III", Journal of Computational Physics, Vol. 71, pp. 231-303.

Jiang,G-S and Wu, C-C., 1999, "A High-Order WENO Finite Difference Scheme for the Equations of Ideal Magnetohydrodynamics", Journal of Computational Physics, Vol. 150, pp. 561-594.

Leonard, B.P., 1988, "Simple high-accuracy resolution program for convective modeling of discontinuities", International Journal for Numerical Methods in Fluids, Vol. 8, pp. 1291-1318.

LeVeque, R.J., 2002, "Finite volumes methods for hyperbolic problems", Press Syndicate of the University of Cambridge.

Lima, G.A.B., 2010, Desenvolvimento de estratégias de captura de descontinuidades para leis de conservação e problemas relacionados em dinâmica dos fluidos, Master's thesis, Instituto de Ciências Matemáticas e de Computação - ICMC/USP.

Liu, X-D., Osher, S. and Chan, T., 1994, "Weighted essentially non-oscillatory schemes", Journal of Computational Physics, Vol. 115, pp. 200-212.

Taylor, G.I., 1974, "Low-Reynolds number flows", National Committee for Fluid Mechanics Films, *Illustrated experiments in fluid mechanics*.

8. Responsibility notice

The authors are the only responsible for the printed material included in this paper.